Desalination and Water Treatment
www.deswater.com

doi:10.5004/dwt.2019.24604

166 (2019) 1–8
October

Investigating the effect of inhomogeneous fixed charge distribution on dielectric exclusion in nanofiltration membranes

Yunjie Zhu[a,b], Haochen Zhu[a,b,*], Aihua Li[a,b], Guangming Li[a,b,*], Zhaohuan Mai[c], Yuliang Gu[d]

[a]*State Key Laboratory of Pollution Control and Resources Reuse, College of Environmental Science and Engineering, Tongji University, 1239 Siping Rd., Shanghai 200092, China, email: 249761317@qq.com (Y. Zhu), ligm@tongji.edu.cn (G. Li)*
[b]*Shanghai Institute of Pollution Control and Ecological Security, Shanghai 200092, P. R. China, email: haochen_zhu@tongji.edu.cn (H. Zhu), 359847042@qq.com (A. Li)*
[c]*Institute of Energy Conversion, Jiangxi Academy of Sciences, Nanchang 330096, China, email: vivianmzh@hotmail.com (Z. Mai)*
[d]*National Engineering Research Center of Urban Water Resources Shanghai National Engineering Research Center of Urban Water Resources Co., Ltd, email: gylqcs@163.com (Y. Gu)*

Received 5 March 2019; Accepted 22 June 2019

ABSTRACT

Nanofiltration has been applied as a promising way in water treatment because of its special separation mechanisms. Most thin-film polyamide nanofiltration membranes obtained by inter facial polymerization possess active layer containing a mine and carboxylic acid groups that are distributed in a highly non-uniform fashion, leading to an inhomogeneous fixed charge distribution. This work is a theoretical research to investigate the impact of inhomogeneous fixed charge distribution on dielectric exclusion in negatively charged nanofiltration membranes. NaCl rejection rate has been computed as a function of different pore radius, feed flow concentration and dielectric constant inside the pore for various inhomogeneous charge distributions with an identical average volume charge density. It has been shown that the difference of rejection performance for fixed charge distributions changes with the variation of pore radius and feed concentration. This phenomenon is related with the electric field behavior determined by functional groups, which also affects the ion partitioning at the solution/membrane interface as well. The dielectric exclusion is therefore affected by the inhomogeneous fixed charge distribution at relatively low pore radius and low feed flow concentration in this work. Thus, the dielectric effect promotes the electrolyte rejection performance differently for fixed charge distributions studied in this work. Conclusions drawn in this work are also likely to benefit the comprehension of separation mechanism of polyamide membranes in nanofiltration process and is valuable for the development of membrane fabrication process on membrane structure and functional group distribution.

Keywords: Nanofiltration; Modeling; Charge distribution; Dielectric exclusion; Rejection performance

1. Introduction

In recent decades, Nanofiltration has been applied as a promising way in water treatment because of its special separation mechanisms. High-solute rejection and low-energy consumption is its major advantage in seawater and brackish water desalination, pure water and waste water treatment [1–3]. Nanofiltration is a pressure driven membrane process, which possess pore size of 0.5–2.0 nm which corresponds to molecular weight cut-off (MWCO) of 100–500 Da and its operation pressure is lower than reverse osmosis and higher than ultra filtration [4–7].

Most thin-film polyamide nanofiltration membranes obtained by inter facial polymerization possess active layer

*Corresponding author.

1944-3994 / 1944-3986 © 2019 Desalination Publications. All rights reserved.

containing a mine and carboxylic acid groups that are distributed in a highly non-uniform fashion [1,8]. Freger et al. have investigated thin-film composite polyamide NF membranes by tangential and transversal characterization techniques (i.e. tangential streaming potential measurements and TEM) and demonstrated that the polymer density and charge are distributed in a highly nonuniform fashion across the active polyamide layer, which contributes a negatively charged outer region sitting on top of an inner region possessing a positive charge density [9,10]. This is also further proved by Pacheco and Pinnau [11]. Wang et al. investigated the electrostatic effect, dictated by the membrane surface potential, on salt rejection to consider the effect of co-existence of negative and positive charges on membrane surface in a non-uniform distribution. The enhanced shielding effect and the complexation of counter ions and groups clearly explained the difference of rejection performance between ions with different valency [12]. Zhu et al. theoretically investigated the effect ascribed to the varied fixed charge density with different electrolyte types and demonstrated that the variation of membrane fixed charge density has a significant effect on electrolytes retention, especially on asymmetric electrolytes [13–15]. The inhomogeneous fixed charge distribution generates a varying electric field along the nanopores and leads to a competition between co ion and counter ion, which is significant for the determination of ion rejection performance [16]. The pore shape also affects the nanopore volume charge density over the thickness of active layer. Beatrice et al. found the hourglass nanopores have better salt rejection performance than conical or cylindrical nanopores due to the stronger electric field arising through the hourglass-shape nanopores in the case of electrically-driven ion transport [17,18]. However, these investigations only focus on electric characteristics to explain ion separation performance while the dielectric exclusion is rarely discussed.

The dielectric exclusion is one of the most important separation mechanisms [19]. It was firstly considered by Gluekauf and then has been discussed for many times since Yaroshchuk firstly suggested the effect of ion interactions with polarization charges or "image forces" at the solution/membrane interface may cause dielectric exclusion [19–24]. This phenomenon is induced at the solvent-membrane surface because of the interaction between ions and membrane materials with different dielectric constant. However, in strongly charged small pores, the interaction between counter ions and fixed charge would lead to the the screening of image force [23]. Born effect is proposed as an appropriate engineering calculation of dielectric exclusion mechanism for nanofiltration membranes in engineering calculation [25,26]. Based on the ion hydration shell, the Born effect was proposed to consider the dehydration and solvation energy barrier due to the change of dielectric constant inside the confined nanopore during the entry of ions at the membrane/solution interface [27,28].

Déon et al. investigated the heterogeneous charge distribution along the membrane pores by means of adsorption isotherms to describe the salts rejection. The decrease of the dielectric constant inside the pore is affected by ion charge and the electrolyte concentration [29]. Silva et al. found a more accurate prediction of nanofiltration separation performance with the variation of volume charge density described as Freundlich charge isotherm and the relative permittivity [27,30–32]. The inhomogeneous fixed charge distribution has been proved to affect the ion transport in nanopores, which leads to different rejection performances of electrolytes. However, no theoretical research investigates the ion transport performance on the variation of fixed charge density over the thickness of active layer under consideration of dielectric exclusion. In addition, both electrostatic repulsion and dielectric exclusion are relevant to ion charge so that the variation of volume charge density is necessary to be discussed synthetically in a steric-electric-dielectric separation theory to reflect the contribution of Donnan effect and its relationship to dielectric exclusion.

The purpose of this work is to investigate the effect of inhomogeneous fixed charge distribution on dielectric exclusion in nanofiltration membranes. The theoretical research is implemented with the description of ion transport through nanopores based on the Poisson-Nernst-Planck theory combined with the Navier-Stokes equation [15,22,33–38]. The dielectric exclusion is calculated as an interfacial partitioning at the inlet and outlet of nanopores [21]. The type of membrane charge is completely negative and NaCl rejection rate has been computed as a function of different pore radius, feed flow concentration and dielectric constant inside the pore for homogeneous fixed charge distribution and various inhomogeneous charge distributions with an identical average volume charge density.

2. Theoretical aspects

In this work, the cylindrical shape is considered in the theoretical investigation of the ion transport (Fig. 1). The solution/membrane interface and the membrane/solution interface are marked as "$0^-|0^+$" and "$L^-|L^+$" to present the inlet and outlet of a pores. The arrow across the pore means the direction of flow. The position inside the pore is marked as "z/L". "ε_p" and "ε_b" represent the dielectric constant of solution inside the pore and bulk solution, respectively. The effect of image forces is neglected and the Born effect is the only dielectric mechanism discussed in this work. Concentration polarization is generally considered as a reversible process that is determined by velocity, pulsation or electric field. It contributes more problematic membrane fouling and mitigates the permeate flux and rejection performance [38,39]. The bulk solutions are assumed to be ideal and extremely stirred therefore the polarization phenomena at the membrane surface is not considered in this work.

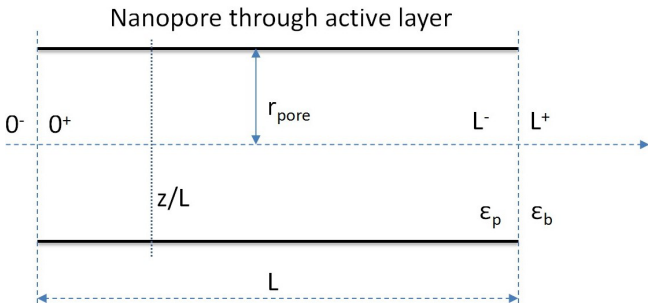

Fig. 1. Representation of a nanopore in active layer.

The expressions of partitioning, ion transport and the analysis of electrolyte rejection rates are listed in Table 1 and the meaning of each symbol is listed in symbol lists. To correspond to the average nanofiltration membrane structural features, the pore radius is set at 0.66 nm and the thickness to porosity ratio (x/A_k) of the skin layer is set at 4.8 μm which corresponds to the average structural features of commercial nanofiltration membranes [5,40,41]. The temperature is 298K [42].

For the sake of clarity, the NaCl is the only electrolyte investigated in this work and the diffusion coefficient of cation and anion is $1.334 \times 10^{-5}\,cm^2\,s^{-1}$ and $2.032 \times 10^{-5}\,cm^2\,s^{-1}$, respectively [43] and we only consider membranes are negatively charged. Therefore, three types of inhomogeneous fixed charge distributions have been presented with volume charge density variation along the nanopore (namely (a) tanh, (b) linear, (c) hyperbolic) in the present work to compare with homogeneous fixed charge distribution. For "hyperbolic" and "linear" fixed charge distribution have been already investigated in pioneer works [13,33]. As mentioned above, the influence of inhomogeneous fixed charge distribution under consideration of dielectric effects is yet not well understood. The "hyperbolic" distribution has a highly charged entrance while the fixed charge density is extremely decreased in the inner part of the nanopore. The "linear" distribution possesses the constant variation of fixed charge density along the pore length. The fixed charge density of "tanh" distribution at the entrance and exit of the

Table 1
Major expressions of ion transport description within the pores

Transport equation	
The modified extended Nernst-Planck equation to describe ion transport in nanopore	$j_i = -K_{i,d}D_{i,\infty}\frac{dc_i}{dx} - \frac{z_i c_i K_{i,d} D_{i,\infty}}{RT}F\frac{d\psi}{dx} + K_{ic}c_i\frac{J_v}{A_k}\left(x = \frac{z}{L}, 0 < x < 1\right)$
Concentration gradient inside the nanopore	$\frac{dc_i}{dx} = \frac{J_V}{K_{i,d}D_{i,\infty}A_k}\left(K_{i,c}c_i - c_i\left(L^+\right)\right) - \frac{z_i F c_i}{RT}\frac{d\psi}{dx}$
Navier-Stokes equation for calculation of influence of electrical double layer on hydrodynamics fluid according to fluid velocity	$-\Delta P + \eta\nabla^2 u - F\sum_i c_i z_i \nabla\psi = 0$
Calculation of local electric potential inside the pore with Poisson equation	$\nabla^2\psi = -\frac{F}{\varepsilon_0\varepsilon_r}\sum_i c_i z_i$
Electroneutrality conditions inside the pores	$\sum z_i c_i(x) + X = 0 (0 < x < 1)$
Fixed charge concentration	$X(x) = \frac{2\sigma(x)}{Fr_p}$
The axial electric field along the pore length	$E(x) = -\frac{d\psi(x)}{d(x)} = -\frac{\sum_i\left(\frac{z_i J_v}{K_{i,d}D_{i,\infty}A_k}\right)\left(K_{i,c}c_i(x) - c_i\left(L^+\right)\right) - \left(\frac{dX(x)}{d(x)}\right)}{\left(\frac{F}{RT}\right)\sum_i c_i(x)z_i^2}$
Partitioning equations	$\frac{c_i,\left(0^+\right)}{c_i,\left(0^-\right)} = \varphi_i\exp\left(-z_i\Delta\psi_{D,(0^+\|0^-)}\right)\exp\left(-\Delta W_{i,Born}\right)$
The partitioning of ions at the membrane/solution interfaces	$\frac{c_i,\left(L^-\right)}{c_i,\left(L^+\right)} = \varphi_i\exp\left(-z_i\Delta\psi_{D,(L^-\|L^+)}\right)\exp\left(-\Delta W_{i,Born}\right)$
Born effect	$\Delta W_{i,Born} = \frac{\left(z_i e\right)^2}{8\pi\varepsilon_0 kTr_{i,cav}}\left(\frac{1}{\varepsilon_p} - \frac{1}{\varepsilon_b}\right)$
Analysis of electrolyte rejection rates	$R = 1 - \frac{c_i,\left(0^-\right)}{c_i,\left(L^+\right)}$

nanopore is the same as "linear" distribution while "tanh" distribution possesses a sharp decrease of fixed charge density in the inner part of the nanopore [15].

The expressions of all the distribution types are listed as follows:

f(homo) = –10;

f(linear) = 20x – 20;

f(tanh) = –10 (–1 + 2/(1 + exp(100(x – 0.5)))) – 10;

f(hyperbolic) = –10/(0.0745 + 4x)

The 2–dimensional graphic expression of "tanh", "linear" and "hyperbolic" variation of local charge density along the pore length can be found in Fig. 2. The average charge density over the active layer thickness of each distribution is 10 mmol/L. The value of local charge density for each fixed charge distribution type at the entrance is –10 mmol/L (homo), –20 mmol/L (tanh), –20 mmol/L (linear), and –134 mmol/L (hyperbolic), respectively. The difference of three inhomogeneous fixed charge distribution is that i) the value of volume charge density of linear and tanh are identical at the inlet and outlet while linear has a smoother variation over the active layer thickness, ii) Hyperbolic has an extremely higher fixed charge density at the inlet.

3. Results and discussion

In order to verify the appropriate pore radius with the presence of significant effect of inhomogeneous fixed charge distribution under consideration of dielectric exclusion, Fig. 3 depicts the variation of the rejection rate versus the nanopore radius for different fixed charge distribution under consideration of steric hindrance, electric exclusion and dielectric exclusion [44]. The rejection rates decrease as the pore radius increases because of the weakened influence of steric hindrance, electric exclusion and dielectric exclusion.

For pore radius is bigger than 1.1 nm, the rejection performance of tanh and linear fixed charge distribution are identical and are both better than hyperbolic and homogeneous fixed charge distribution. It indicates that the fixed charge density at the pore entrance cannot effectively affect the rejection performance at pore radius larger than 1 nm while the fixed charge density in the inner part of the nanopore is more significant (i.e. The sharp decrease of volume charge density in hyperbolic distribution contributes the lowest charge intensity. The sequence of average charge density for the middle part of the inner part of the nanopore is $X_{hyperbolic} < X_{homo} < X_{tanh} = X_{linear}$). In fact, the pore radius of most nanofiltration membranes is smaller than 1 nm (for instance, the pore radius for the membranes NF 90, NF 270 and ESNA1–K1 are 0.3 nm, 0.4 nm and 0.47 nm, respectively [41,45,46]). In this study, the theoretical retention performance of inhomogeneous fixed charge distribution is better than homogeneous fixed charge distribution at pore radius less than 1.1 nm. It indicates that the volume

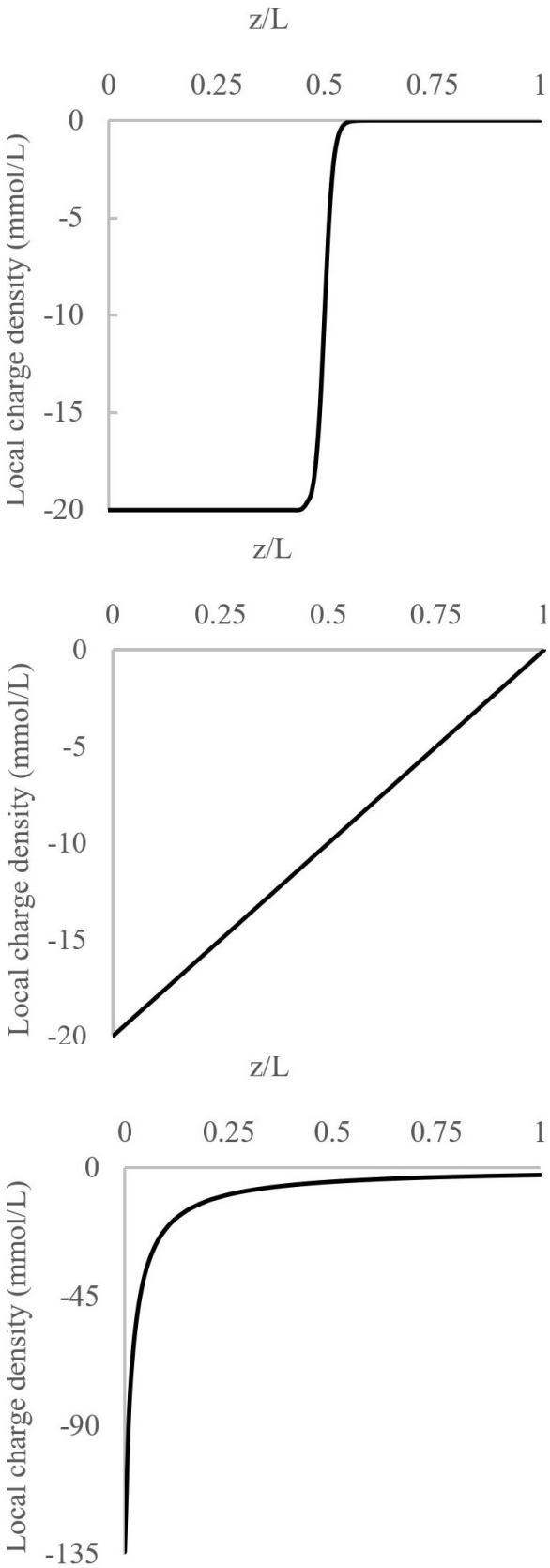

Fig. 2. Three types of inhomogeneous fixed charge distribution along the pore length: (a) tanh; (b) linear; (c) hyperbolic.

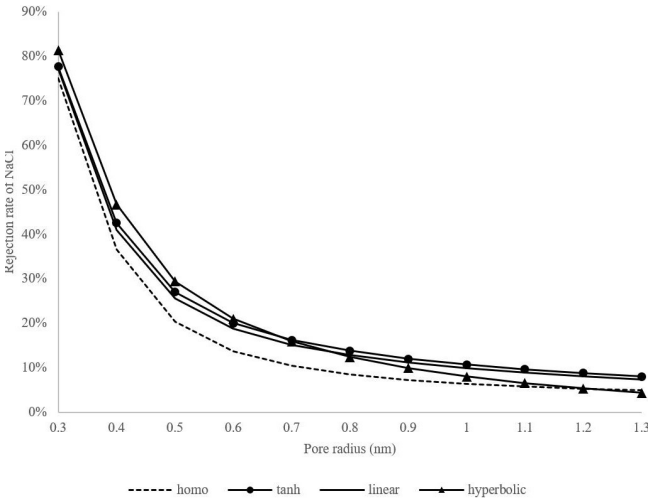

Fig. 3. Variation of the rejection rate of NaCl vs. the pore radius for the various fixed charge distribution. x/A_k = 4.8 μm, ε_p = 70, $C_{NaCl} = 2 \times 10^{-3}$ mol/L, $J_v = 2 \times 10^{-6}$ m/s.

charge density at the pore inlet significantly affects the rejection performance when pore radius is small (The value of local charge density for each fixed charge distribution type at the entrance is –10 mmol/L (homo), –20 mmol/L (tanh), –20 mmol/L (linear), and –134 mol/L (hyperbolic), respectively) [13].

In addition, it must be stressed that the consideration of dielectric exclusion on rejection rate of all the fixed charge distributions only enhance the total rejection performance and will not change the sequence of rejection performance for each fixed charge distribution at high feed concentration (i.e. $C_{NaCl} = 2 \times 10^{-3}$ mol/L in this study). This is due to that the contribution of inhomogeneous fixed charge distribution is overcompensated by counter ions to maintain the electro neutrality. Thus, the electro migration decreases and the influence of variation of volume charge density in the inner part of the nanopore is reduced. In contrast, the influence of inhomogeneous fixed charge distribution on dielectric exclusion is different at low feed concentration (i.e. $C_{NaCl} \leq 0.3 \times 10^{-3}$ mol/L in this work), which affects the separation performance. Therefore, dielectric exclusion is disregarded in previous theoretical researches focusing on inhomogeneous fixed charge distribution [14,15]. The relationship between feed concentration and the influence of inhomogeneous fixed charge distribution is investigated in Fig. 4.

Fig. 4 presents the variation of rejection rate of NaCl versus the solute concentration for different fixed charge distribution under consideration of steric hindrance, electric exclusion and dielectric exclusion, in which the retention performance of inhomogeneous fixed charge distributions is better than homogeneous fixed charge distribution at different solute concentration at pore radius equals 0.66 nm. For the sake of clarity, it is worth mentioning that the ion hydration of NaCl has been regarded as a constant state so that the quantitative relationship between dielectric exclusion and fixed charge distribution will not be influenced by activity quotient. The difference of rejection performance between inhomogeneous and homogeneous fixed charge distribution increases as the feed flow concentration

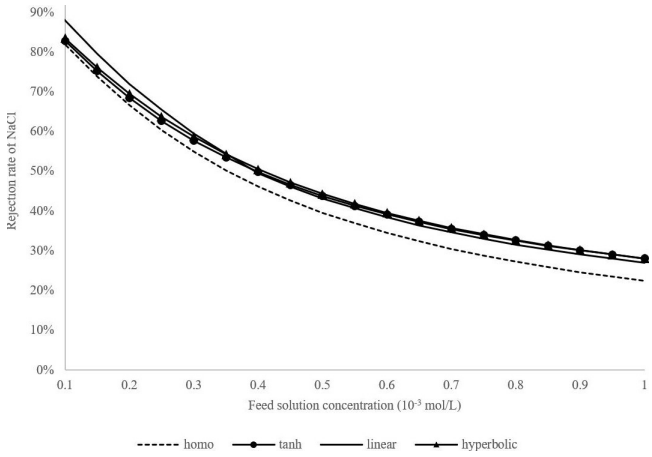

Fig. 4. Variation of the rejection rate of NaCl vs. the concentration of feed flow for the different fixed charge distribution. r_p = 0.66 nm, x/A_k = 4.8 μm, ε_p = 70, $J_v = 2 \times 10^{-6}$ m/s.

increases. It indicates that the effect of electric exclusion is significant to rejection performance due to the influence of the variation of fixed charge density inside the membrane pores. However, the rejection performance of linear fixed charge distribution is apparently better than other inhomogeneous fixed charge distribution at low solute concentration because of the influence of dielectric exclusion (i.e. $C_{NaCl} < 0.4 \times 10^{-3}$ mol/L).

This can be proved by Fig. 5, which presents the difference of rejection rate between consideration with or without dielectric exclusion. The difference of rejection rate at solute concentration less than 0.3×10^{-3} mol/L reflects the dominant role of dielectric effect on rejection performance. In this case, the rejection rate growth of linear fixed charge distribution is better than others while tanh and hyperbolic distribution is lower than homogeneous fixed charge distribution. It suggests that the linear distribution supports a stronger dielectric exclusion than others. Corresponding to rejection performance in Fig. 4, when solute concentration

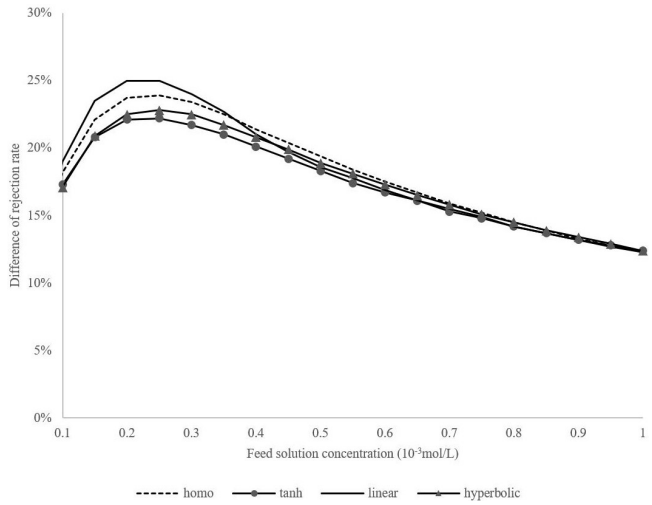

Fig. 5. The difference of rejection rate between consideration with or without dielectric exclusion. r_p = 0.66 nm, x/A_k = 4.8 μm, ε_p = 70, $J_v = 2 \times 10^{-6}$ m/s.

is bigger than 0.3 × 10^{-3} mol/L, the difference of rejection rate of all the types of fixed charge distribution is reduced. It indicates that the increase of electrolyte concentration screens the electrostatic interaction between ions and the membrane fixed charge [22,47,48]. Therefore, the influence of dielectric exclusion is more competitive than electric exclusion and the influence of variation of fixed charge density on dielectric exclusion is reduced.

The rejection performance of linear fixed charge distribution can be explained by local electric field that the dielectric exclusion is strongly affected by inhomogeneous fixed charge distribution at low concentration (Fig. 6). The electro migration is more significant than convection when permeate volume flux is low enough (J_v = 2 × 10^{-6} m/s) for charged membranes [49]. Based on the expression of the axial electric field along the pore length, the electric field can be determined by the volume flux and fixed charge distribution. Therefore, the maximum value and position of the electric field peak inside the pore for fixed charge distributions are different. The hyperbolic distribution possesses an intensive volume charge density at the inlet of the nanopore so that the coions are significantly prevented to enter the nanopore [50–52]. However, the intensity of electric field for hyperbolic distribution is weaker than tanh and linear, the strength of preventing coions passing through the nanopore is therefore reduced. In contrast, the electric field strength of tanh distribution increases sharply in the transition zone to limit the transfer of counter ions through the middle of the nanopore to maintain the electro neutrality. The peak value of electric field for tanh distribution is also higher than hyperbolic distribution. Therefore, the tanh charge distribution is expected to have similar rejection as hyperbolic charge distribution.

In comparison, since the linear distribution possesses an intensive electric field at the end of the pore and the peak value of linear distribution is much larger than tanh, hyperbolic and homogeneous distribution (Fig. 6), it strongly prevents the electro migrative flux of counter ions from moving toward the low–pressure side [33,34]. Therefore, the linear distribution is proved to have a more significant influence on counter ions and the ion partitioning at the outlet of the pore(i.e. membrane/solution interface) of inhomogeneous fixed charge distributions are not identical. Thus, for concentration is lower than 0.35 mol/m^3, the rejection performance follows the series $R_{linear} > R_{tanh} \approx R_{hyperbolic} > R_{homo}$. Therefore, the dielectric exclusion is proved to be tightly associated with the variation of volume charge density at low solute concentration.

In addition, the rejection rate for three inhomogeneous fixed charge distributions coincide after 0.35 mol/L feed concentration and are all better than homogeneous fixed charge distribution (Fig. 4). It suggests that the volume charge density at the pore inlet affects the electric exclusion to contribute a different rejection performance. In contrast, as the feed concentration increases, the contribution of inhomogeneous fixed charge distribution is overcompensated to maintain the electro neutrality. Thus, the electro migration decreases progressively with respect to convection and diffusion, and the influence of variation of volume charge density in the inner part of the nanopore is reduced. Therefore, the influence of electric field distribution along the nanopore on ion partitioning at the solution/membrane interface is mitigated.

The relationship of the rejection performance and the intensity of dielectric exclusion is presented in Fig. 7. When Born effect is not considered (i.e. $\varepsilon_p = \varepsilon_b$ = 80), the rejection performance of linear, tanh and hyperbolic are close and are all better than homogeneous distribution. This is attributed to the influence of inhomogeneous fixed charge distribution [13]. The rejection rate of all distribution types rises as the intensity of Born effect grows (i.e. the difference between ε_p and ε_b becomes bigger). The rejection rate of inhomogeneous and homogeneous fixed charge distribution tends to be closer due to the strong competitiveness of dielectric exclusion based on the different dielectric constant between bulk solution and solution inside the pore becomes larger and thus the effect of inhomogeneous fixed charge distribution is mitigated.

However, the linear distribution shows a better rejection performance than others for dielectric constant value inside the nanopores less than 50. This is attributed to the sharp peak of electric field with tanh distribution in transition regime does not affect the ion partitioning at the solution/

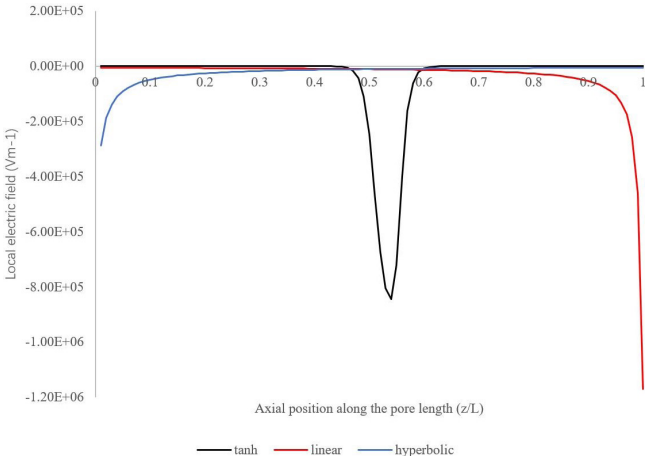

Fig. 6. Local electric field inside membrane pores. The variation of fixed charge density correspond to those shown in Fig. 2. r_p = 0.66 nm, x/A_k = 4.8 μm, ε_p = 70, C_{NaCl} = 0.3 × 10^{-3} mol/L, J_v = 2 × 10^{-6} m/s.

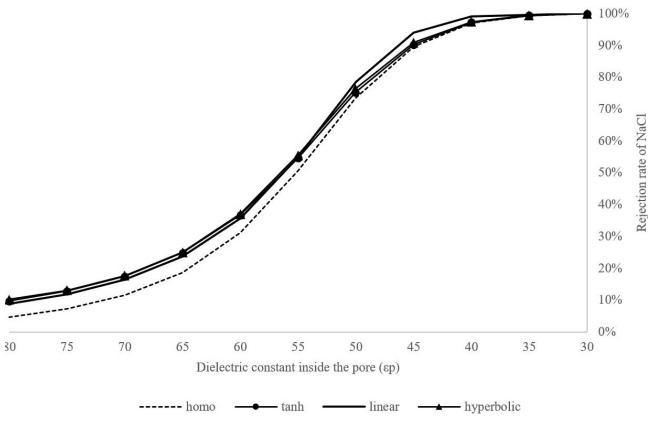

Fig. 7. The rejection rate of NaCl vs. dielectric constant inside the pore for 4 types of fixed charge distribution under consideration of dielectric exclusion. Whereas, r_p = 0.66 nm, x/A_k = 4.8 μm, C_{NaCl} = 2 × 10^{-3} mol/L, J_v = 2 × 10^{-6} m/s.

membrane interface and the peak value of electric field for tanh and hyperbolic distribution are both lower than linear distribution and the linear fixed charge distribution possesses an intensive electric field strength at the end of the membrane pores to promote the ion partitioning at the membrane/solution interface (L–|L+). It suggests that the significant influence of inhomogeneous fixed charge distribution on dielectric exclusion to affect the rejection performance.

4. Conclusion

This work is a theoretical research to investigate the impact of inhomogeneous fixed charge distribution on dielectric exclusion in negatively charged nanofiltration membranes at low volume flux. NaCl rejection rate has been computed as a function of different pore radius, feed flow concentration and dielectric constant inside the pore for various inhomogeneous charge distributions with an identical average volume charge density.

The competitive relationship between electric exclusion and dielectric exclusion on rejection performance is determined by the extent of the screening of the electrostatic interaction between ions and the membrane fixed charge.

In addition, the inhomogeneous fixed charge distribution contributes to the variation of axial electric field strength inside the membrane pores to determine the transfer of coions and counter ions, which affects the ion partitioning at the solution/membrane interface as well. The dielectric exclusion is therefore affected by the inhomogeneous fixed charge distribution at low pore radius and low feed flow concentration. However, the intensive Born effect contributes the dominant role of dielectric exclusion and the influence of the variation of volume charge density is reduced. Results presented in this work suggests that focusing on the distribution of functional groups in development of the polyamide nanofiltration membrane fabrication process can promote the rejection performance.

Acknowledgement

This work was supported by Major Science and Technology Program for Water Pollution Control and Treatment (2017ZX07207004) and National Natural Science Foundation of China (21603164 & 21567009).

Symbols

A_k — Membrane porosity
c_i — Solute concentration
$D_{i,\infty}$ — Diffusion coefficient in the bulk solution ($m^2 s^{-1}$)
$E(x)$ — Electric potential inside the pore (V m^{-1})
e — Elementary charge
F — Faraday constant
j_i — Molar flux of ion i (mol $m^{-2} s^{-1}$)
J_v — Permeate volumetric flux (m s^{-1})
$K_{i,c}$ — Convection hindrance factor for the ion i
$K_{i,d}$ — Diffusion hindrance factor for the ion i
k — Boltzmann constant
P — Pressure (N m^{-2})
R — Ideal gas constant
$r_{i,cav}$ — Cavity radius of ions
T — Temperature (K)
uc — Solute velocity (m s^{-1})
$W_{i,Born}$ — Dimensionless excess solvation energy due to Born effect for ion i
$X(x)$ — Membrane volumetric charge density (mmol L^{-1})
z — Axial position along the pore
z_i — Charge of ion i (valence)
ε_0 — Vacuum permittivity ($J^{-1} C^2 m^{-1}$)
ε_r — Solution dielectric constant
ε_β — Dielectric constant of the bulk
ε_π — Dielectric constant inside the pore
η — Solvent viscosity (N s m^{-2})
ψ — Local electric potential inside the nanopore (V)

References

[1] Y. Ji, W. Qian, Y. Yu, Q. An, L. Liu, Y. Zhou, Recent developments in nanofiltration membranes based on nanomaterials, Chin. J. Chem. Eng., 25 (2017) 1639–1652.
[2] M.A. Abdel-Fatah, Nanofiltration systems and applications in wastewater treatment: Review article, Ain Shams Eng., in press (2018).
[3] A.W. Mohammad, Y.H. Teow, W.L. Ang, Y.T. Chung, D.L. Oatley–Radcliffe, N. Hilal, Nanofiltration membranes review: Recent advances and future prospects, Desalination, 356 (2015) 226–254.
[4] R.J. Petersen, Composite reverse osmosis and nanofiltration membranes, J. Membr. Sci., 83 (1993) 81–150.
[5] O. Labban, T.H. Chong, J.H.L. V, Design and modeling of novel low–pressure nanofiltration hollow fiber modules for water softening and desalination pretreatment, Desalination, 439 (2018) 58–72.
[6] C.S. Ong, W.J. Lau, A.F. Ismail, Treatment of dyeing solution by NF membrane for decolorization and salt reduction, Desal. Water Treat., 50 (2012) 245–253.
[7] D. Dolar, K. Košutić, D. Ašperger, Influence of adsorption of pharmaceuticals onto RO/NF membranes on their removal from water, Water Air Soil Poll., 224 (2012).
[8] V. Freger, S. Srebnik, Mathematical model of charge and density distributions in inter facial polymerization of thin films, J. Appl. Polym. Sci., 88 (2003) 1162–1169.
[9] d.V. Freger, Nanoscale Heterogeneity of polyamide membranes formed by inter facial polymerization, Langmuir, 19 (2003) 4791–4797.
[10] S. Bason, Y. Oren, V. Freger, Characterization of ion transport in thin films using electrochemical impedance spectro scopyII: examination of the polyamide layer of RO membranes, J. Membr. Sci., 302 (2007) 10–19.
[11] F.A. Pacheco, I. Pinnau, M. Reinhard, J.O. Leckie, Characterization of isolated polyamide thin films of RO and NF membranes using novel TEM techniques, J. Membr. Sci., 358 (2010) 51–59.
[12] Z. Wang, K. Xiao, X.–m. Wang, Role of coexistence of negative and positive membrane surface charges in electrostatic effect for salt rejection by nanofiltration, Desalination, 444 (2018) 75–83.
[13] H. Zhu, A. Szymczyk, B. Balannec, Influence of an inhomogeneous membrane charge density on the rejection of electrolytes by NF membranes entile article, Desal. Water Treat., 18 (2010) 182–186.
[14] H. Zhu, A. Szymczyk, B. Balannec, On the salt rejection properties of nanofiltration polyamide membranes formed by inter facial polymerization, J. Membr. Sci., 379 (2011) 215–223.

[15] A. Szymczyk, H. Zhu, B. Balannec, Ion rejection properties of nanopores with bipolar fixed charge distributions, J. Phys. Chem., B 114 (2010) 10143–10150.
[16] F.G. Donnan, Theory of membrane equilibria and membrane potentials in the presence of non-dialysing electrolytes. A contribution to physical–chemical physiology, J. Membr. Sci., 100 (1995) 45–55.
[17] B. Balannec, A. Ghoufi, A. Szymczyk, Nanofiltration performance of conical and hourglass nanopores, J. Membr. Sci., 552 (2018) 336–340.
[18] S. Tseng, S.C. Lin, C.Y. Lin, J.P. Hsu, Influences of cone angle and surface charge density on the ion current rectification behavior of a conical nanopore, J. Phys. Chem. C., 120 (2016) 25620–25627.
[19] S. Bandini, D. Vezzani, Nanofiltration modeling: the role of dielectric exclusion in membrane characterization, Chem. Eng. Sci., 58 (2003) 3303–3326.
[20] A.E. Yaroshchuk, Dielectric exclusion of ions from membranes, Adv. Colloid Interf. Sci., 85 (2000) 193–230.
[21] A. Szymczyka, N. Fatin-Rouge, P. Fievet, C. Ramseyer, A. Vidonne, Identification of dielectric effects in nanofiltration of metallic salts, J. Membr. Sci., 287 (2007) 102–110.
[22] A. Szymczyk, P. Fievet, Investigating transport properties of nanofiltration membranes by means of a steric, electric and dielectric exclusion model, J. Membr. Sci., 252 (2005) 77–88.
[23] D.L. Oatley, L. Llenas, N.H.M. Aljohani, P.M. Williams, X. Martínez-Lladó, M. Rovira, J.d. Pablo, Investigation of the dielectric properties of nanofiltration membranes, Desalination, 315 (2013) 100–106.
[24] A. Yaroshchuk, M.L. Bruening, E. Zholkovskiy, Modelling nanofiltration of electrolyte solutions, Adv. Colloid Interface Sci., 268 (2019) 39–63.
[25] D.L. Oatley, L. Llenas, R. Perez, P.M. Williams, X. Martinez–Llado, M. Rovira, Review of the dielectric properties of nanofiltration membranes and verification of the single oriented layer approximation, Adv Colloid Interface Sci., 173 (2012) 1–11.
[26] D. Vezzani, S. Bandini, Donnan equilibrium and dielectric exclusion for of nanofiltration membranes, Desalination, 149 (2002) 477–483.
[27] W.R. Bowen, J.S. Welfoot, Modelling the performance of membrane nanofltration – critical assessment and model development, Chem. Eng. Sci., 57 (2002) 1121–1137.
[28] T. Tsuru, S.-i. Nakao, S. Kimura, Calculation of ion rejection by extended Nernst Planck equation with charged reverse osmosis membranes for single and mixed electrolyte solutions, J. Chem. Eng. J. pn., 24 (1991) 511–517.
[29] S. Déon, A. Escoda, P. Fievet, A transport model considering charge adsorption inside pores to describe salts rejection by nanofiltration membranes, Chem. Eng. Sci., 66 (2011) 2823–2832.
[30] V. Silva, Á. Martín, F. Martínez, J. Malfeito, P. Prádanos, L. Palacio, A. Hernández, Electrical characterization of NF membranes. A modified model with charge variation along the pores, Chem. Eng. Sci., 66 (2011) 2898–2911.
[31] J.I. Calvo, A. Hernández, P. Prádanos, F. Tejerina, Charge adsorption and zeta potential in cyclopore membrane, J. Membr. Sci., 181 (1996) 399–412.
[32] V. Silva, M. Montalvillo, F.J. Carmona, L. Palacio, A. Hernández, P. Prádanos, Prediction of single salt rejection in nanofiltration membranes by independent measurements, Desalination, 382 (2016) 1–12.
[33] A. Szymczyk, H. Zhu, B. Balannec, Pressure-driven ionic transport through nanochannels with in homogenous charge distributions, Langmuir, 26 (2010) 1214–1220.
[34] A. Szymczyk, C. Labbez, P. Fievet, A. Vidonne, A. Foissy, J. Pagetti, Contribution of convection, diffusion and migration to electrolyte transport through nanofiltration membranes, Adv. Colloid Interface Sci., 103 (2003) 77–94.
[35] J. Fang, B. Deng, Rejection and modeling of arsenate by nanofiltration: Contributions of convection, diffusion and electro migration to arsenic transport, J. Membr. Sci., 453 (2014) 42–51.
[36] J. Garcia-Aleman, J.M. Dickson, Mathematical modeling of nanofiltration membranes with mixed electrolyte solutions, J. Membr. Sci., 235 (2004) 1–13.
[37] D.W. Nielsen, G. Jonsson, Bulk-phase criteria for negative ion rejection in nanofiltration of multicomponent salt solutions, Sep. Sci. Technol, 29 (1994) 1165–1182.
[38] S.S. Vasan, R.W. Field, Z. Cui, A Maxwell-Stefan-Gouy-Debye model of the concentration profile of a charged solute in the polarisation layer, Desalination, 192 (2006) 356–363.
[39] S.S. Vasan, C.D. Bain, R.W. Field, Z. Cui, A Maxwell-Stefan-Derjaguin-Grahame model of the concentration profile of a charged solute in the polarisation layer, Desalination, 200 (2006) 175–177.
[40] W.R. Bowen, A.W. Mohammad, A theoretical basis for specifying nanofiltration membranes – Dye/salt/water streams, Desalination, 117 (1998) 257–264.
[41] S.S. Wadekar, R.D. Vidic, Influence of active layer on separation potentials of nanofiltration membranes for inorganic ions, Environ. Sci. Technol., 51 (2017) 5658–5665.
[42] Y. Roy, D.M. Warsinger, J.H. Lienhard, Effect of temperature on ion transport in nanofiltration membranes: Diffusion, convection and electro migration, Desalination, 420 (2017) 241–257.
[43] W.R. Bowen, A.W. Mohammad, N. Hilal, Characterisation of nanofiltration membranes for predictive purposes – use of salts, uncharged solutes and atomic force microscopy, J. Membr. Sci., 126 (1997) 91–105.
[44] J. Luo, Y. Wan, Effects of pH and salt on nanofiltration—a critical review, J. Membr. Sci., 438 (2013) 18–28.
[45] L.D. Nghiem, A.I. Schäfer, M. Elimelech, Removal of natural hormones by nanofiltration membranes: Measurement, modeling, and mechanisms, Environ. Sci. Technol., 38 (2004) 1888–1896.
[46] K.-L. Tung, Y.-C. Jean, D. Nanda, K.-R. Lee, W.-S. Hung, C.-H. Lo, J.-Y. Lai, Characterization of multilayer nanofiltration membranes using positron annihilation spectroscopy, J. Membr. Sci., 343 (2009) 147–156.
[47] S. Bandini, J. Drei, D. Vezzani, The role of pH and concentration on the ion rejection in polyamide nanofiltration membranes, J. Membr. Sci., 264 (2005) 65–74.
[48] S. Bandini, C. Mazzoni, Modelling the amphoteric behaviour of polyamide nanofiltration membranes, Desalination, 184 (2005) 327–336.
[49] P. Fievet, C. Labbez, A. Szymczyk, A. Vidonne, A. Foissy, J. Pagetti, Electrolyte transport through amphoteric nanofiltration membranes, Chem. Eng. Sci., 57 (2002) 2921–2931.
[50] P. Árki, C. Hecker, G. Tomandl, Y. Joseph, Streaming potential properties of ceramic nanofiltration membranes – Importance of surface charge on the ion rejection, Sep. Purif. Technol., 212 (2019) 660–669.
[51] D.-X. Wang, M. Su, Z.-Y. Yu, X.-L. Wang, M. Ando, T. Shintani, Separation performance of a nanofiltration membrane influenced by species and concentration of ions, Desalination, 175 (2005) 219–225.
[52] M. Teixeira, M. Rosa, M. Nystrom, The role of membrane charge on nanofiltration performance, J. Membr. Sci., 265 (2005) 160–166.